

Free massive particles with total energy $E < mc^2$ in curved spacetimes

Jorge Castiņeiras

Instituto de Física Teórica, Universidade Estadual Paulista, Rua Pamplona 145, 01405-900, São Paulo, São Paulo, Brazil

Luis C. B. Crispino

Departamento de Física, Universidade Federal do Pará, Campus Universitário do Guamá, 66075-900, Belém, Pará, Brazil

George E. A. Matsas

Instituto de Física Teórica, Universidade Estadual Paulista, Rua Pamplona 145, 01405-900, São Paulo, São Paulo, Brazil

Daniel A. T. Vanzella

Physics Department, University of Wisconsin-Milwaukee, 1900 E Kenwood Blvd., Milwaukee, WI 53211

We analyze *free elementary particles* with rest mass m and *total energy* $E < mc^2$ in the Rindler wedge, outside Reissner-Nordstrom black holes and in the spacetime of relativistic (and non-relativistic) stars, and use Unruh-DeWitt-like detectors to calculate the associated particle detection rate in each case. The (mean) particle position is identified with the spatial average of the excitation probability of the detectors, which are supposed to cover the whole space. Our results are shown to be in harmony with General Relativity classical predictions. Eventually we reconcile our conclusions with Earth-based experiments which are in good agreement with $E \geq mc^2$.

04.60.+n

I. INTRODUCTION

The standard theory of quantum fields uses the fact that the Minkowski spacetime is maximally symmetric. The linear three momenta (k^x, k^y, k^z) associated with the translational isometries on the spacelike hypersurfaces $t = \text{const}$ constitutes a suitable set of quantum numbers to label free particles, where we are assuming here that (t, x, y, z) are the usual Minkowski coordinates. In this simple case, the dispersion relation $E \equiv \hbar\omega = \sqrt{|\mathbf{k}c|^2 + m^2 c^4}$ imposes a simple constraint between the particle mass m , momentum \mathbf{k} and energy E , and, thus, free particles with well defined linear momenta must have total energy $E \geq mc^2$. Because Earth-based particle experiments assume in general the detection of asymptotic free states in Minkowski spacetime, the possibility of measuring particles with total energy

$$E < mc^2 \quad (1.1)$$

is usually neglected. Moreover, in the classical context of General Relativity, the detection *in loco* of *point* particles satisfying Eq. (1.1) by direct capture is ruled out by the fact that an observer with four-velocity u^μ intercepting a

particle with four-momentum $k^\mu = mv^\mu$ ascribes to the particle an energy $E = mv^\mu u_\mu \geq mc^2$. On the other hand, it is well known that, unlike standard Quantum Field Theory in flat spacetime, the field quantization carried over curved (stationary) backgrounds does not lead in general to any dispersion relation for the energy and other quantum numbers, avoiding thus the flat spacetime constraint $E \geq mc^2$. This can be understood by recalling that the concept of *point particle* finds no room in the context of Quantum Field Theory. Two main questions are raised, then, by the discussion above: Given a stationary spacetime (i) *what is the minimum energy $E_{\min} \equiv \hbar\omega_{\min}$ allowed for a particle?* and (ii) *what is the probability density associated with the detection of particles with $E \in [E_{\min}, mc^2)$ at different space points?*

We analyze the questions above in the context of Quantum Theory of Linear Fields in Curved Spacetimes where the normal modes associated with our particles are seen as free. In order to define clearly what we mean by “observing a particle” we use Unruh-DeWitt detectors (endowed with an internal structure defined by a density of states). Our results are shown to be in agreement with General Relativity predictions concerning the position of

particles with $E < mc^2$ as defined by the same fiducial observers who proceed to the field quantization and with Earth-based experiments which usually assume $E \geq mc^2$.

The paper is organized as follows. In Section II we consider a two-dimensional Schwarzschild black hole which maintains a close relationship with the Rindler wedge where a full analytical investigation can be carried out. This section is important as a “theoretical laboratory” for the next ones and to provide a better understanding of some phenomena as, e.g., the decay of uniformly accelerated protons [1]. This is so because the proton interaction with *massive* particles possessing energy $E < mc^2$ plays an important rôle according to coaccelerated observers with the proton. In Section III we investigate the questions (i) and (ii) outside Reissner-Nordstrom black holes. We discuss, in particular, the agreement of our results with General Relativity. In Section IV we consider relativistic (and non-relativistic) stars. This case is qualitatively different from the earlier ones because the energy spectrum of particles with $E < mc^2$ is discrete. This fact is a reflection of the nonexistence of event horizons in the star spacetime. We show eventually that for Earth-based experiments $E_{\min} \approx mc^2$, as expected. Our final remarks are made in Section V. We will assume hereafter natural units, $\hbar = c = G = 1$, unless stated otherwise.

II. DETECTION OF MASSIVE PARTICLES IN A TWO-DIMENSIONAL BLACK HOLE-LIKE SPACETIME

Let us begin considering the line element of a two-dimensional Schwarzschild spacetime:

$$ds^2 = (1 - 2M/r) dt^2 - (1 - 2M/r)^{-1} dr^2. \quad (2.1)$$

Eq. (2.1) can be seen as describing a two-dimensional black hole with mass M . Close to the horizon, $r \approx 2M$, Eq. (2.1) can be written as

$$ds^2 = (\rho/4M)^2 dt^2 - d\rho^2, \quad (2.2)$$

where $\rho(r) \equiv \sqrt{8M(r - 2M)}$. (Note that in these coordinates the horizon is at $\rho = 0$.) Line element (2.2) is associated with the Rindler wedge (which is a globally hyperbolic spacetime) provided that $0 < \rho < +\infty$ and $-\infty < t < +\infty$. The advantage of considering spacetime (2.2) rather than (2.1) is three-fold: first it has the main relevant features (for our purposes) of the two-dimensional Schwarzschild spacetime (the fact that they differ asymptotically will not be important at this point),

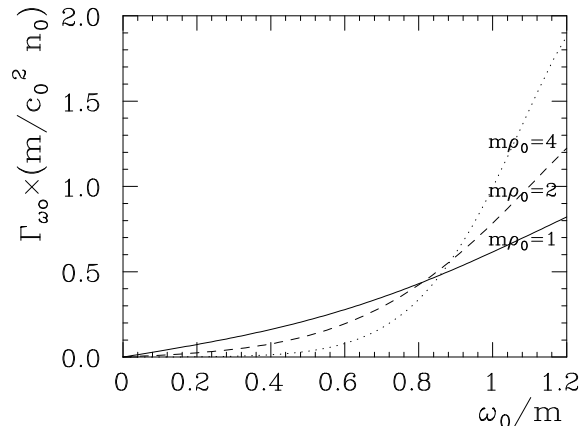


FIG. 1. We plot the detection rate Γ_{ω_0} as a function of the ω_0/m ratio for observers at different points ρ_0 . For observers far away from the horizon, there is a strong detection damping.

second it provides a better understanding of some phenomena occurring in uniformly accelerated frames and third it allows a completely analytic discussion.

Let us now consider in this spacetime a free scalar field $\hat{\Phi}(x)$ with mass m . The positive-frequency solutions of the Klein-Gordon equation $(\square + m^2)u_\omega(x^\mu) = 0$ can be written as $u_\omega(x^\mu) \equiv \psi_\omega(\rho)e^{-i\omega t}$ where

$$-\frac{d^2\psi_\omega}{d\rho^2} + V_{\text{eff}}^{\text{RW}}\psi_\omega(\rho) = \omega^2\psi_\omega(\rho). \quad (2.3)$$

Here $x = 4M \ln(\rho/4M)$ and $V_{\text{eff}}^{\text{RW}} = (4M)^{-2}\rho^2 m^2$. Note that the effective potential grows unboundedly at the infinity. By solving Eq. (2.3), we obtain

$$u_\omega(x^\mu) = \sqrt{(4M/\pi^2) \sinh(4\pi M\omega)} K_{4iM\omega}(m\rho)e^{-i\omega t}, \quad (2.4)$$

where $K_\nu(x)$ is the modified Bessel function and we have orthonormalized $u_\omega(x)$ according to the Klein-Gordon inner product [2]- [4]. Note that $\omega \in (0, +\infty)$, i.e., there are massive Rindler particles with arbitrarily small energies.

Next, the field is expanded in terms of positive- and negative-frequency modes as usually:

$$\hat{\Phi}(x) = \int_0^{+\infty} d\omega [\hat{a}_\omega u_\omega(x) + H.c.], \quad (2.5)$$

where the annihilation and creation operators satisfy $[\hat{a}_\omega, \hat{a}_{\omega'}^\dagger] = \delta(\omega - \omega')$. Since $\partial_t u_\omega = -i\omega u_\omega$, the *fiducial observer* with respect to whom the quantization is

performed is the one at $\rho = \rho_0 = 4M$, whose proper time is t [see Eq. (2.2)]. The Rindler vacuum $|0\rangle$ is defined from $\hat{a}_\omega|0\rangle = 0$.

Now, we introduce an Unruh-DeWitt detector [5] described by a localized monopole $\hat{m}(s)$ with proper time s and worldline $z^\mu = z^\mu(s)$. Let \hat{H} be the detector free Hamiltonian acting as $\hat{H}|E\rangle = E|E\rangle$ on the detector energy eigenstates $|E\rangle$ and $\hat{m}(s) = e^{i\hat{H}s}\hat{m}(0)e^{-i\hat{H}s}$. We will denote by $|E_G\rangle$ the detector ground state and assume $E_G \equiv 0$. The excited states of the detector will be ruled by some (normalized) density of states $\beta_{E_0}(E)$ peaked at $E = E_0$ and satisfying

$$\int_0^{+\infty} dE \beta_{E_0}(E) = 1. \quad (2.6)$$

The simplest choice is $\beta_{E_0}(E) = \delta(E - E_0)$ which characterizes a single excited-state detector. This will be enough in the black hole cases but not in the relativistic star one where we have to deal with particles with discrete energy spectra. For the later case it is more convenient to consider

$$\begin{aligned} \beta_{E_0}(E) = & (n/E_0) [\Theta(E - E_0 + E_0/2n) \\ & - \Theta(E - E_0 - E_0/2n)], \end{aligned} \quad (2.7)$$

where $n = \text{const.} \gg 1$ and $\Theta(x)$ is the step function. We note that Eq. (2.7) satisfies Eq. (2.6) and the useful property $\beta_{cE_0}(cE) = c^{-1}\beta_{E_0}(E)$ for $c \in \mathbf{R}$. Moreover, we can recover the single excited-state detector in the $n \rightarrow +\infty$ limit, since $\lim_{n \rightarrow +\infty} \beta_{E_0}(E) = \delta(E - E_0)$. Once the detector is defined, we couple it to a massive scalar field $\hat{\Phi}(x^\mu)$ through the interaction action

$$\hat{S}_I = \int_{-\infty}^{+\infty} ds c_0 \hat{m}(s) \hat{\Phi}[x^\mu(s)], \quad (2.8)$$

where c_0 is a small coupling constant.

Let us now ask to our fiducial observer what is the total probability per (detector) proper time $\Gamma_\omega(\rho_d) \equiv P_\omega(\rho_d)/s_d^{\text{tot}}$ of detecting a particle at some point ρ_d with energy ω . The excitation amplitude (at the tree level) $\mathcal{A}_\omega^{\text{det}} \equiv \langle 0| \otimes \langle E|\hat{S}_I|E_G\rangle \otimes |\omega\rangle$ associated with the particle detection can be shown to be

$$\begin{aligned} \mathcal{A}_\omega^{\text{det}} = & 4 c_0 \sqrt{M \sinh(4\pi M\omega)} K_{4iM\omega}(m\rho_d) \\ & \times \delta(E - 4M\omega/\rho_d), \end{aligned} \quad (2.9)$$

where the detector selectivity was chosen such that $\langle E|m(0)|E_G\rangle \equiv 1$. The detection rate is thus given by

$$\begin{aligned} \Gamma_\omega(\rho_d) = & \frac{1}{s_d^{\text{tot}}} \int_0^{+\infty} dE \beta_{E_0}(E) \int_0^{+\infty} d\omega' |\mathcal{A}_{\omega'}^{\text{det}}|^2 F_\omega(\omega') \\ = & \frac{2c_0^2}{\pi} \sinh(\pi E_0 \rho_d) \rho_d K_{iE_0 \rho_d}^2(m\rho_d) F_\omega\left(\frac{E_0 \rho_d}{4M}\right), \end{aligned} \quad (2.10)$$

where we have chosen the density of states $\beta_{E_0}(E) = \delta(E - E_0)$ and $F_\omega(\omega')$ characterizes a mixed state peaked at the particle energy ω with the property that $F_\omega(\omega) = n_0 = \text{const.}$ for every ω . (One can avoid the introduction of mixed states by considering the detection of wave packets, as shown below.) Now, we carefully adjust the detector at each point ρ_d to *maximize* the detection probability (2.10). This is achieved by properly tuning its energy excitation gap: $E_0 = 4M\omega/\rho_d$ (note that E_0 and ω are related by a red-shift factor, as it should be). Hence Eq. (2.10) becomes

$$\Gamma_\omega(\rho_d) = \frac{2c_0^2}{\pi} n_0 \sinh(4\pi M\omega) \rho_d K_{4iM\omega}^2(m\rho_d). \quad (2.11)$$

Now, we may wonder what is the probability rate Γ_{ω_0} that a massive state $|\omega_0\rangle$ be measured by our observer at ρ_0 in the particular case where the detector is carried by our experimentalist, i.e., $\rho_d = \rho_0$ (and we recall that in the Rindler wedge $M = \rho_0/4$). In Fig. (1) we plot

$$\Gamma_{\omega_0} = \frac{2c_0^2}{\pi} n_0 \sinh(\pi \rho_0 \omega_0) \rho_0 K_{i\rho_0 \omega_0}^2(m\rho_0), \quad (2.12)$$

as a function of ω_0/m . We clearly note that the farther away the observer is from the horizon, the steeper the detection damping for $\omega_0/m < 1$.

Next, let us define from Eq. (2.11) the normalized probability density

$$d\mathcal{P}_\omega/d\rho_d \equiv \Gamma_\omega(\rho_d) / \int_0^{+\infty} \Gamma_\omega(\rho'_d) d\rho'_d. \quad (2.13)$$

$(d\mathcal{P}_\omega/d\rho_d)d\rho_d$ is the probability that a particle with energy ω be found between ρ_d and $\rho_d + d\rho_d$. We see from Fig. (2) that observers far away from the horizon will only be able to interact with the ‘‘tail’’ of the ‘‘wave functions’’ associated with particles with small ω/m .

The physical content carried out by Eq. (2.13) can be reproduced by considering wave packets (rather than mixed states) as follows. Let us represent a particle with typical energy ω through a wave packet defined as

$$|\phi_\omega\rangle \equiv \int_0^{+\infty} d\omega' G_\omega(\omega') \hat{a}_{\omega'}^\dagger |0\rangle, \quad (2.14)$$

where $G_\omega(\omega')$ is a peaked function at $\omega' = \omega$ and $\int_0^{+\infty} d\omega' |G_\omega(\omega')|^2 = 1$ in order that $\langle \phi_\omega | \phi_\omega \rangle = 1$. The *total* probability for detecting $|\phi_\omega\rangle$ (at the tree level) at some ρ_d between the constant-coordinate-time hypersurfaces $t = \text{const} \rightarrow -\infty$ and $t = \text{const} \rightarrow +\infty$ is $\tilde{\mathcal{P}}_\omega^{\text{wp}}(\rho_d) = |\langle 0| \otimes \langle E_0|\hat{S}_I|E_G\rangle \otimes |\phi_\omega\rangle|^2$, where we should tune the detector as before, $E_0 = 4M\omega/\rho_d$, to maximize

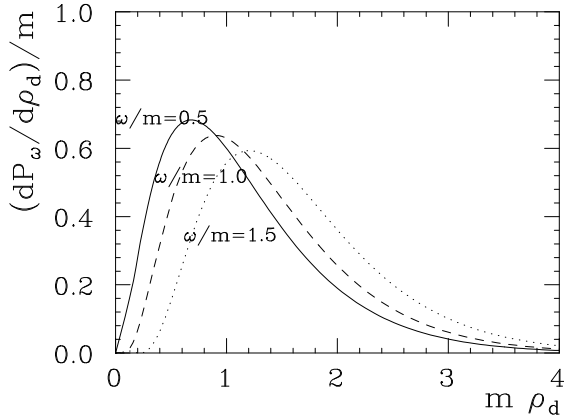


FIG. 2. We plot the probability density $d\mathcal{P}_\omega/d\rho_d$ for different ω/m ratios, where we have assumed $Mm = 1/4$. We note that the smaller the ω/m ratio, the closer to the horizon (in average) the particle lies, where the “gravitational potential” is stronger.

its detection probability. In order to obtain the probability between the constant-proper-time hypersurfaces $s = \text{const} \rightarrow -\infty$ and $s = \text{const} \rightarrow +\infty$, we must multiply both sides by the red-shift factor $4M/\rho_d$:

$$\mathcal{P}_\omega^{wp}(\rho_d) = 4c_0^2 |G_\omega(\omega)|^2 \sinh(4\pi M\omega) \rho_d K_{4iM\omega}^2(m\rho_d), \quad (2.15)$$

where $G_\omega(\omega) = \text{const}$. Note that Eqs. (2.15) and (2.11) differ only by a (dimensional) constant factor. Thus by replacing $\Gamma_\omega(\rho_d)$ by $\mathcal{P}_\omega^{wp}(\rho_d)$ in Eq. (2.13), we obtain the same probability density $d\mathcal{P}_\omega/d\rho_d$.

Now, in order to interpret Eq. (2.13) on General Relativity bases, let us first consider a row of detectors each of them lying at different ρ_d and define the *average detection position*

$$\langle \rho_d \rangle \equiv \int_0^{+\infty} d\rho_d \rho_d d\mathcal{P}_\omega/d\rho_d. \quad (2.16)$$

By using Eq. (2.13), we obtain

$$\langle \rho_d \rangle = \frac{\pi \tanh(4\pi M\omega)(64M^2\omega^2 + 1)}{64mM\omega} \approx \pi M\omega/m \quad (\omega \gg a), \quad (2.17)$$

where $a \equiv 1/4M$ is the proper acceleration of the fiducial observer.

Now, from General Relativity, a classical particle with mass m lying at rest at some point ρ_p has, according

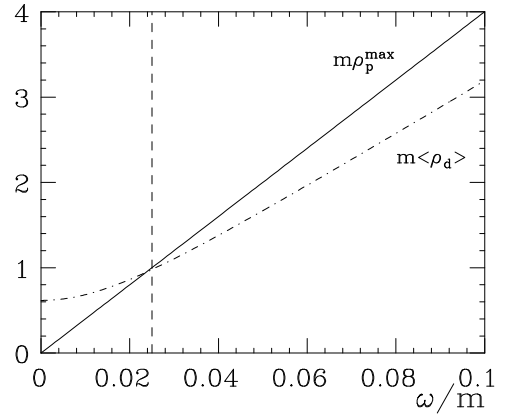


FIG. 3. $\langle \rho_d \rangle$ is shown to be smaller than $\rho_p^{\text{max}} \equiv 4M\omega/m$ in the “high-frequency” regime $\omega > (4M)^{-1}$ (i.e., at the right of the vertical broken line) just as expected. (We have assumed here $mM = 10$ but this nice agreement is verified for any mM .)

to our fiducial observer at $\rho_0 = 4M$, total energy $\omega = m\rho_p/4M$. By considering that the particle may have in addition some kinetic energy, the total energy would be $\omega \geq m\rho_p/4M$. By inverting this equation, we obtain

$$\rho_p \leq \rho_p^{\text{max}} \equiv 4M\omega/m, \quad (2.18)$$

which is expected to agree with $\langle \rho_d \rangle$, i.e., $\langle \rho_d \rangle \leq \rho_p^{\text{max}}$, at least in the “high-frequency” regime $\omega \gg a$ (where the quantum and classical behaviors may be compared). This conclusion is indeed in agreement with Eqs. (2.17) and (2.18) (see also Fig. 3). The smaller the ω/m ratio, the more likely to detect the particle closer to the horizon where the “effective gravitational potential” decreases its total energy.

III. DETECTION OF MASSIVE PARTICLES OUTSIDE REISSNER-NORDSTROM BLACK HOLES

Let us consider now the line element of a globally-hyperbolic spherically-symmetric static spacetime

$$ds^2 = f(r)dt^2 - h(r)dr^2 - r^2(d\theta^2 + \sin^2\theta d\varphi^2), \quad (3.1)$$

where we assume that we are restricted to a region ($f(r) > 0$) where the Killing field $(\partial_t)^\mu$ is *timelike*. We may cast the positive-frequency solutions of the Klein-Gordon equation $(\square + m^2)u_{\omega lm}^\alpha(x) = 0$ in the form ($l \in \mathbf{N}$, $-l \leq m \leq l$)

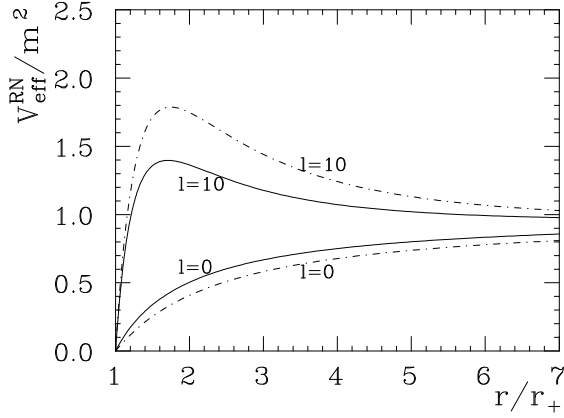


FIG. 4. The scattering potential is plotted for $l = 0$ and $l = 10$. Full and dashed lines are related with $Q = 0$ and $Q = 0.9M$, respectively. $V_{\text{eff}}^{\text{RN}}$ vanishes at the horizon and tends asymptotically to m^2 . We note that the larger the angular momentum, the higher the potential and the more difficult to find a particle with $\omega/m < 1$ far from the horizon. (We have assumed here $mM = 2$.)

$$u_{\omega l m}^{\alpha}(x) = \sqrt{\frac{\omega}{\pi}} \frac{\psi_{\omega l}^{\alpha}(r)}{r} Y_{lm}(\theta, \varphi) e^{-i\omega t}, \quad (3.2)$$

where $\psi_{\omega l}^{\alpha}(r)$ satisfies

$$-\sqrt{\frac{f}{h}} \frac{d}{dr} \left(\sqrt{\frac{f}{h}} \frac{d}{dr} \right) \psi_{\omega l}^{\alpha}(r) + V_{\text{eff}} \psi_{\omega l}^{\alpha}(r) = \omega^2 \psi_{\omega l}^{\alpha}(r) \quad (3.3)$$

with the following scattering potential:

$$V_{\text{eff}} \equiv \left[\frac{\sqrt{f/h}}{r} \frac{d\sqrt{f/h}}{dr} + \frac{l(l+1)f}{r^2} + m^2 f \right]. \quad (3.4)$$

The label α was introduced to distinguish between the two independent solutions of the radial equation (3.3).

Outside a static black hole ($r > r_+$) with mass M and charge Q ($Q \leq M$), we have $f^{\text{RN}}(r) = 1/h^{\text{RN}}(r)$, where

$$f^{\text{RN}}(r) = (1 - r_+/r)(1 - r_-/r) > 0 \quad (3.5)$$

and $r_{\pm} \equiv M \pm \sqrt{M^2 - Q^2}$. (The label ‘‘RN’’ is a shortcut for Reissner-Nordstrom.) In this case, the scattering potential

$$V_{\text{eff}}^{\text{RN}} = \left[1 - \frac{2M}{r} + \frac{Q^2}{r^2} \right] \left[\frac{2M}{r^3} - \frac{2Q^2}{r^4} + \frac{l(l+1)}{r^2} + m^2 \right] \quad (3.6)$$

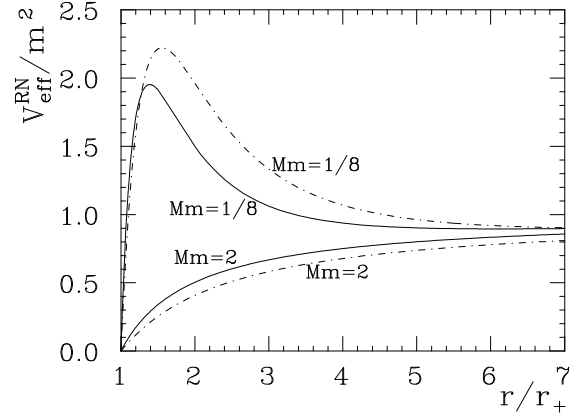


FIG. 5. The scattering potential is plotted for $mM = 1/8$ and $mM = 2$. Full and dashed lines are related with $Q = 0$ and $Q = 0.9M$, respectively. We note that the larger mM , the more favorable to detect particles with $\omega/m < 1$. (Here we have assumed $l = 0$.)

vanishes at the horizon, $r = r_+$, and tends to m^2 asymptotically [see Fig. (4)]. Thus, only ‘‘outgoing’’ particles, $\alpha \equiv \rightarrow$, from the white hole horizon \mathcal{H}^- will be able to comply Eq. (1.1). (Eventually they will be totally reflected to the black hole horizon \mathcal{H}^+ .) *Incoming* particles from \mathcal{J}^- , $\alpha \equiv \leftarrow$, will necessarily have $\omega \geq m$. [The case $\omega = m$ is somewhat subtler and will not be considered here (see Refs. [6]- [7] for the case $\omega = m = 0$).] Let us note that the larger the l , the higher the centrifugal barrier of the potential [see Fig. (4)]. As a consequence, particles with $l \gg 1$ which are found to verify Eq. (1.1) will be necessarily restricted to a close neighborhood around the horizon, where the gravitational field is strong enough to compensate the angular momentum effect. Hence, in order to find particles satisfying Eq. (1.1) ‘‘relatively’’ far from the horizon, we will focus on particles with $l = 0$.

For chargeless black holes, the local extrema of the scattering potential can be analytically determined. For the case $l = 0$ and $Mm < 1/4$, we have

$$r_1 = \frac{1}{m} \left(\sqrt{3} \sin \frac{\xi}{3} - \cos \frac{\xi}{3} \right) \text{ and } r_2 = \frac{2}{m} \cos \frac{\xi}{3}, \quad (3.7)$$

where r_1 and r_2 are associated with a local maximum and minimum ($r_1 < r_2$), respectively, and $\xi \equiv \pi - \arctan[\sqrt{1 - 16(mM)^2/(4mM)}]$. For the case $l = 0$ and $Mm > 1/4$ there are no local extrema [see Fig. (5)]. For $Mm = 1/4$, $r_1 = r_2$ is an inflection point and $V_{\text{eff}}^{\text{RN}}|_{r=r_1, r_2} = 3m^2/4$. For a black hole with $M \geq 3M_{\odot}$

and a particle with mass $m \geq m_{e^-}$, we have $Mm \geq 10^{16}$. This is why we will focus our simulations on values $Mm > 1/4$. An analytic investigation of the local extrema when $Q \neq 0$ is not possible since $dV_{\text{eff}}^{\text{RN}}/dr = 0$ results in a full fifth-order algebraic equation but it can be seen numerically [see, e.g., Figs. (4) and (5)] that the presence of charge does not change significantly the form of the potential $V_{\text{eff}}^{\text{RN}}(r/r_+)$.

By using the coordinate transformation [6]

$$r \rightarrow x = y + \frac{y_-^2 \ln(y - y_-) - y_+^2 \ln(y - y_+)}{y_- - y_+}, \quad (3.8)$$

where $y \equiv r/2M$ and $y_{\pm} \equiv r_{\pm}/2M$, we can rewrite Eq. (3.3) as

$$-\frac{d^2 \psi_{\omega l}^{\alpha}}{dx^2} + 4M^2 V_{\text{eff}}^{\text{RN}}(x[y(r)]) \psi_{\omega l}^{\alpha} = 4M^2 \omega^2 \psi_{\omega l}^{\alpha}. \quad (3.9)$$

Thus, close to and far from the horizon, we can write the outgoing $\psi_{\omega l}^{\alpha}$ functions as ($\omega \geq 0$, i.e., $\omega_{\min} = 0$)

$$\psi_{\omega l}^{\rightarrow}(x) \approx A_{\omega l}^{\rightarrow} \begin{cases} e^{2iM\omega x} + \mathcal{R}_{\omega l}^{\rightarrow} e^{-2iM\omega x} & (x < 0, |x| \gg 1) \\ \mathcal{T}_{\omega l}^{\rightarrow} e^{2iM\omega x} & (x \gg 1) \end{cases} \quad (3.10)$$

and the incoming ones as ($\omega \geq m$, i.e., $\omega_{\min} = m$)

$$\psi_{\omega l}^{\leftarrow}(x) \approx A_{\omega l}^{\leftarrow} \begin{cases} \mathcal{T}_{\omega l}^{\leftarrow} e^{-2iM\omega x} & (x < 0, |x| \gg 1) \\ e^{-2iM\omega x} + \mathcal{R}_{\omega l}^{\leftarrow} e^{2iM\omega x} & (x \gg 1), \end{cases} \quad (3.11)$$

where $\tilde{\omega} \equiv \sqrt{\omega^2 - m^2}$. For $\omega \geq m$, $|\mathcal{R}_{\omega l}^{\leftarrow}|^2$, $|\mathcal{R}_{\omega l}^{\rightarrow}|^2$ and $|\mathcal{T}_{\omega l}^{\leftarrow}|^2$, $|\mathcal{T}_{\omega l}^{\rightarrow}|^2$ can be seen as reflection and transmission coefficients, respectively, satisfying the probability conservation equations

$$|\mathcal{R}_{\omega l}^{\rightarrow}|^2 + \frac{\tilde{\omega}}{\omega} |\mathcal{T}_{\omega l}^{\rightarrow}|^2 = 1 \quad \text{and} \quad |\mathcal{R}_{\omega l}^{\leftarrow}|^2 + \frac{\omega}{\tilde{\omega}} |\mathcal{T}_{\omega l}^{\leftarrow}|^2 = 1. \quad (3.12)$$

For $\omega < m$, the outgoing modes fade exponentially far away from the horizon and $|\mathcal{R}_{\omega l}^{\rightarrow}| = 1$. One of the tests performed to guaranty the reliability of our codes was the verification that Eqs. (3.10)-(3.11) were satisfied (with the appropriate relations for $\mathcal{R}_{\omega l}^{\alpha}$ and $\mathcal{T}_{\omega l}^{\alpha}$) along the numerical calculation.

We normalize $\psi_{\omega l}^{\alpha}$ such that $u_{\omega l m}^{\alpha}$ are Klein-Gordon orthonormalized [2]- [4]:

$$i \int_{\Sigma_t} d\Sigma n^{\mu} \left(u_{\omega l m}^{\alpha} * \nabla_{\mu} u_{\omega' l' m'}^{\alpha'} - u_{\omega' l' m'}^{\alpha'} \nabla_{\mu} u_{\omega l m}^{\alpha} * \right) = \delta_{AA'} \quad (3.13)$$

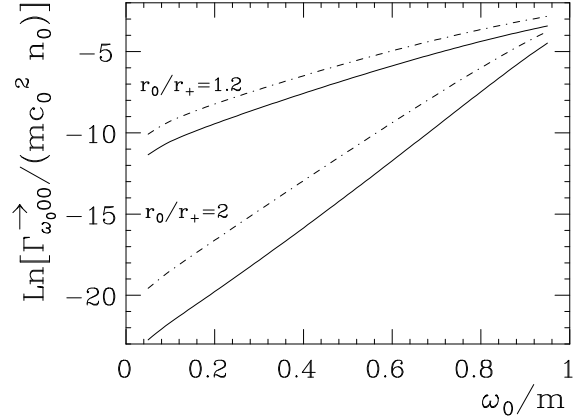


FIG. 6. We plot the detection rate $\Gamma_{\omega_0 0 0}^{\rightarrow}$ as a function of the ω_0/m ratio for observers at different points r_0 . Full and dashed lines are related with $Q = 0$ and $Q = 0.9M$, respectively. The damping in the detection rate is steeper for observers far away from the horizon. (We have assumed here $mM = 2$.)

$$i \int_{\Sigma_t} d\Sigma n^{\mu} \left(u_{\omega l m}^{\alpha} \nabla_{\mu} u_{\omega' l' m'}^{\alpha'} - u_{\omega' l' m'}^{\alpha'} \nabla_{\mu} u_{\omega l m}^{\alpha} \right) = 0, \quad (3.14)$$

where here $\delta_{AA'} \equiv \delta_{\alpha\alpha'} \delta_{ll'} \delta_{mm'} \delta(\omega - \omega')$ and n^{μ} is the future-pointing unit vector normal to the volume element of the Cauchy surface Σ_t . By using Eq. (3.9) to transform the left-hand side of Eq. (3.13) in a surface term, we obtain the normalization constants $A_{\omega l}^{\rightarrow} = (2\omega)^{-1}$ and $A_{\omega l}^{\leftarrow} = (2\sqrt{\omega\tilde{\omega}})^{-1}$ (up to an arbitrary phase). The incoming and outgoing modes are orthogonal to each other with respect to the Klein-Gordon inner product (3.13)-(3.14). This can be seen by choosing $\Sigma_t = \mathcal{H}^- \cup \mathcal{J}^-$ in Eq. (3.13) and recalling that $\psi_{\omega l}^{\rightarrow}(x)$ and $\psi_{\omega l}^{\leftarrow}(x)$ vanish on \mathcal{J}^- and \mathcal{H}^- , respectively.

Next we expand a massive scalar field $\hat{\Phi}(x)$ in terms of positive and negative frequency modes:

$$\hat{\Phi}(x) = \sum_{\alpha=\rightarrow}^{\leftarrow} \sum_{l=0}^{+\infty} \sum_{m=-l}^l \int_{\omega_{\min}}^{+\infty} d\omega [\hat{a}_{\omega l m}^{\alpha} u_{\omega l m}^{\alpha}(x) + \text{H.c.}], \quad (3.15)$$

where $\omega_{\min} = 0$ when $\alpha = \rightarrow$ and $\omega_{\min} = m$ when $\alpha = \leftarrow$. As a consequence of orthonormalizing the normal modes with the Klein-Gordon inner-product, the annihilation $\hat{a}_{\omega l m}^{\alpha}$ and creation $\hat{a}_{\omega l m}^{\alpha\dagger}$ operators satisfy the simple commutation relations

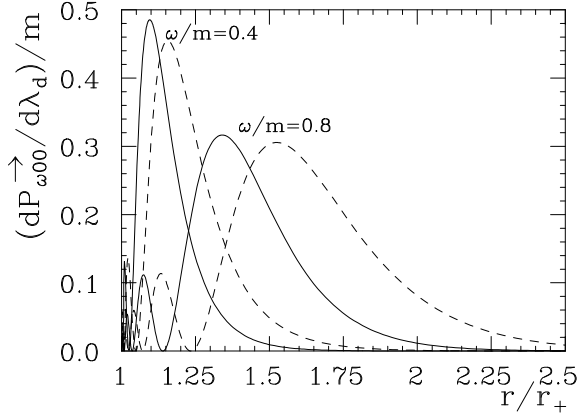


FIG. 7. The probability density $(d\mathcal{P}_{\omega_0 00}^{\rightarrow}/d\lambda_d)/m$ is plotted for $\omega/m = 0.4$ and $\omega/m = 0.8$. Full and dashed lines are related with $Q = 0$ and $Q = 0.9M$, respectively. (Here we have assumed $Mm = 2$.) We note that the smaller the ω/m ratio, the closer to the horizon the particle should be.

$$\left[\hat{a}_{\omega l m}^{\alpha}, \hat{a}_{\omega' l' m'}^{\alpha' \dagger} \right] = \delta_{\alpha\alpha'} \delta_{ll'} \delta_{mm'} \delta(\omega - \omega'). \quad (3.16)$$

The Boulware vacuum $|0\rangle$ is defined by $\hat{a}_{\omega l m}^{\alpha}|0\rangle = 0$ for every α, ω, l and m .

Let us assume an Unruh-DeWitt detector coupled to the massive scalar field as described by the interaction action (2.8). The detection rate (detection probability per detector proper time) of particles with quantum numbers α, ω, l and m (as defined by asymptotic fiducial observers) can be calculated (at the tree level):

$$\Gamma_{\omega l m}^{\alpha} = 2c_0^2 n_0 \omega \sqrt{f^{RN}(r_d)} \frac{|\psi_{\omega l}^{\alpha}(r_d)|^2}{r_d^2} |Y_{lm}(\theta_d, \varphi_d)|^2, \quad (3.17)$$

where $n_0 = F_{\omega}(\omega) = \text{const.}$, we have chosen $\beta_{E_0}(E) = \delta(E - E_0)$ and we have tuned again the energy gap of the detector at each point r_d in order to maximize the detection probability, namely, $E_0 = \omega/\sqrt{f^{RN}(r_d)}$.

As in the case of the Rindler wedge, we may calculate the detection rate $\Gamma_{\omega_0 l m}^{\alpha}$ in the particular case where the massive state $|\alpha \omega_0 l m\rangle$ is defined by an experimentalist lying on the precise location of the detector, i.e., $r_0 = r_d$. In principle, this would require that the scalar field were quantized with respect to a fiducial observer at r_0 (in which case $e^{-i\omega t}$ in Eq. (3.2) would be replaced by $e^{-i\omega\tau}$ with $\tau = \sqrt{f^{RN}(r_0)}t$). It is not difficult to see, however, that $\Gamma_{\omega_0 l m}^{\alpha}$ can be obtained directly from Eq. (3.17) with the following replacements: $r_d \rightarrow r_0$

and $\omega \rightarrow \sqrt{f^{RN}(r_0)}\omega_0$. [One can check this strategy in the Rindler wedge by obtaining directly Eq. (2.12) from Eq. (2.11).] In Fig. (6) we plot $\Gamma_{\omega_0 00}^{\rightarrow}$ as a function of ω_0/m for observers at different locations. (We recall that in four-dimensional spacetimes c_0 is dimensionless, in contrast to the case where the spacetime is two-dimensional.)

Now, let us define from Eq. (3.17) the (scalar) normalized probability density

$$d\mathcal{P}_{\omega l m}^{\alpha}/dV_d \equiv \Gamma_{\omega l m}^{\alpha}(\mathbf{x}_d)/\int \Gamma_{\omega l m}^{\alpha}(\mathbf{x}')dV'. \quad (3.18)$$

Here $(d\mathcal{P}_{\omega l m}^{\alpha}/dV_d)dV_d$ is the probability that a particle with quantum numbers (α, ω, l, m) be found at some spatial point $\mathbf{x}_d = (r_d, \theta_d, \phi_d)$ in a proper volume $dV_d = d\lambda_d r_d^2 \sin\theta_d d\theta_d d\phi_d$, where $d\lambda_d = \sqrt{h^{RN}(r_d)}dr_d$. The proper radial distance can be integrated from the horizon $r = r_+$ as a function of the radial coordinate:

$$\begin{aligned} \lambda(r) &= \int_{r_+}^r dr' \sqrt{h^{RN}(r')} \\ &= r \sqrt{f^{RN}(r)} + M \ln \left[\frac{r + r \sqrt{f^{RN}(r)} - M}{r_+ - M} \right]. \end{aligned} \quad (3.19)$$

Notice that $\lambda = \lambda(r)$ is a regular function except in the case of extreme Reissner-Nordstrom black holes ($Q = M$). From Eq. (3.18), we obtain the radial-distance probability density

$$\frac{d\mathcal{P}_{\omega l m}^{\alpha}}{d\lambda_d} \equiv \frac{\sqrt{f^{RN}(r_d)} |\psi_{\omega l}^{\alpha}(r_d)|^2}{\int_0^{+\infty} d\lambda_d' \sqrt{f^{RN}(r_d')} |\psi_{\omega l}^{\alpha}(r_d')|^2}. \quad (3.20)$$

Note that here $(d\mathcal{P}_{\omega l m}^{\alpha}/d\lambda_d)d\lambda_d$ is the probability of detecting a particle with quantum numbers (α, ω, l, m) inside a shell between λ_d and $\lambda_d + d\lambda_d$. In Fig. (7), we use Eq. (3.20) to plot $d\mathcal{P}_{\omega l m}^{\alpha}/d\lambda_d$ for particles with different ω/m ratios (and $l = 0$). We see that the smaller the ω/m the closer to the black hole horizon the particle will be in average.

Next, in order to determine the mean particle radial distance, we calculate numerically [see Fig. (8)]

$$\langle \lambda_d \rangle \equiv \int_0^{+\infty} d\lambda_d \lambda_d d\mathcal{P}_{\omega l m}^{\alpha}/d\lambda_d. \quad (3.21)$$

Note that modes with $\omega/m \geq 1$ spreads over the whole space and thus $\langle \lambda_d \rangle$ diverges. This is qualitatively different from the Rindler wedge case where the scattering potential grows unboundedly at the infinity what causes the normal modes to vanish asymptotically. As a consequence, at the Rindler wedge, $\langle \rho_d \rangle$ is finite even for $\omega/m > 1$ [see Eq. (2.17)].

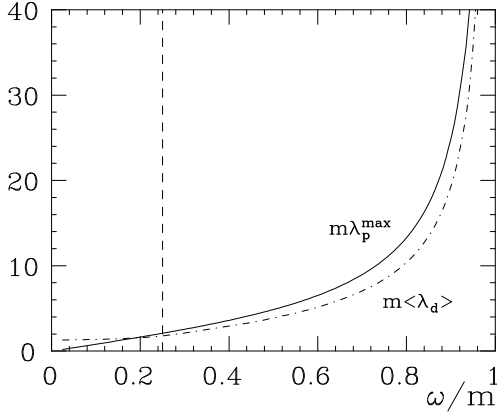


FIG. 8. $\langle \lambda_d \rangle$ is plotted for $\alpha \Rightarrow$ and $l = 0$ and compared with λ_p^{\max} . We see, indeed, that $\langle \lambda_d \rangle < \lambda_p^{\max}$ in the “high-frequency” regime $\omega > r_+^{-1}$ (i.e., at the right of the vertical broken line). (We have assumed here $mM = 2$ and $Q = 0$.)

Now, by repeating our General Relativistic analysis performed in the Rindler wedge case in a more compact way, we obtain that according to (our fiducial) static asymptotic observers a particle with mass m at some point (r_p, θ_p, ϕ_p) with some four-velocity u^μ has total energy $\omega = mu^\mu(\partial_t)_\mu = m\sqrt{f^{\text{RN}}(r_p)}\sqrt{1 + |u^i u_i|} \geq m\sqrt{f^{\text{RN}}(r_p)}$. (The equality holds when the particle is at rest.) By inverting this relation, we obtain that a classical particle with mass m and total energy ω (with $\omega < m$) will be at $r_p \leq r_p^{\max}$, where

$$r_p^{\max} = \frac{M[1 + \sqrt{1 - (1 - \omega^2/m^2)(Q/M)^2}]}{1 - \omega^2/m^2} \quad (3.22)$$

(and $r_p = r_p^{\max}$ only when the particle lies at rest). Because the proper radial distance $\lambda = \lambda(r)$ is a growing monotonic function, $\lambda_p \leq \lambda_p^{\max} \equiv \lambda(r_p^{\max})$. In the “high-frequency” regime, $\omega \gg r_+^{-1}$, we expect as before $\langle \lambda_d \rangle \leq \lambda_p^{\max}$ (see Sec. II). This is indeed verified in Fig. (8).

IV. DETECTION OF MASSIVE PARTICLES AT RELATIVISTIC STARS

Let us consider a static relativistic star with uniform density $\alpha_0 = \text{const}$. The associated line element can be written as in Eq. (3.1) (see Ref. [8]) with

$$f^s(r) = \frac{1}{4} \left(3\sqrt{1 - \frac{2M}{R}} - \sqrt{1 - \frac{2Mr^2}{R^3}} \right)^2 \Theta(R - r) + \left(1 - \frac{2M}{r} \right) \Theta(r - R) \quad (4.1)$$

and

$$h^s(r) = (1 - 2m(r)/r)^{-1} = \left(1 - 2M\frac{r^2}{R^3} \right)^{-1} \Theta(R - r) + \left(1 - \frac{2M}{r} \right)^{-1} \Theta(r - R), \quad (4.2)$$

where $m(r) = 4\pi \int_0^r \alpha_0 r'^2 dr'$. We are using here the label “s” to denote quantities associated with the *star* space-time. In these coordinates, $r = R$ defines the star radius and $M = (4\pi/3)\alpha_0 R^3$ is the star total mass (which, of course, differs from the star total *proper* mass because of the binding energy contribution). Note that for sake of stability, $R > R_c \equiv 9M/4$.

The positive-frequency solutions can be cast in the same form given in Eq. (3.2) where $\psi_{\omega l}^\alpha$ is defined by Eq. (3.3) with $f(r)$ and $h(r)$ given in Eqs. (4.1) and (4.2), respectively. The scattering potential can be obtained by using Eqs. (4.1) and (4.2) in Eq. (3.4):

$$V_{\text{eff}}^s(r) = \left[\frac{M}{R^3} \left(\frac{-9F(R)}{2} + \frac{9}{2} \sqrt{\frac{F(R)}{h^s(r)}} - \frac{1}{h^s(r)} \right) + \frac{1}{4} \left(\frac{l(l+1)}{r^2} + m^2 \right) \left(9F(R) + \frac{1}{h^s(r)} - 6\sqrt{\frac{F(R)}{h^s(r)}} \right) \right] \times \Theta(R - r) + f^s(r) \left(\frac{2M}{r^3} + \frac{l(l+1)}{r^2} + m^2 \right) \Theta(r - R) \quad (4.3)$$

where $F(R) \equiv 1 - 2M/R$. At the star surface the potential has a discontinuity:

$$\lim_{r \rightarrow R^-} V_{\text{eff}}^s(r) = F(R) \left(\frac{l(l+1)}{R^2} - \frac{M}{R^3} + m^2 \right),$$

$$\lim_{r \rightarrow R^+} V_{\text{eff}}^s(r) = F(R) \left(\frac{l(l+1)}{R^2} + \frac{2M}{R^3} + m^2 \right).$$

In Fig. 9 we plot the scattering potential for different star parameters. (Note that the discontinuity of V_{eff}^S at $r/R = 1$ is very small for the parameters chosen in Fig. 9 to be self-evident.) It is interesting to observe that the gravitational field of the Earth is too faint to significantly influence the scattering potential for an electron-mass particle ($m = 0.5 \text{ MeV}$). At the center where the influence would be maximum, we would have for $M = 6 \cdot 10^{27} \text{ g}$

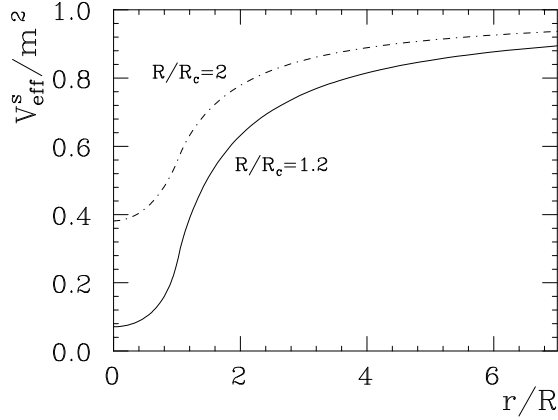


FIG. 9. The scattering potential is plotted for different R/R_c values. We have assumed here $mM = 2$. The denser the star, the larger the influence of the gravitational field. The first eigenfrequencies for these potentials are listed in Tab. I.

(and $l = 0$) that $V_{\text{eff}}^s(r) = m^2(1 - 10^{-48})$ which should be compared with $V_{\text{eff}}^s(r)|_{M=0} = m^2$ obtained in the absence of gravity. Notwithstanding, for quasi-extreme stars ($R \approx R_c$) the scattering potential can be quite affected by the gravitational field (see Fig. 9). Indeed it is possible to devise situations where the gravitational field of a star would be of some importance for particle-physics processes [9].

The normal modes with $\omega < m$ will be bounded states and $\omega_{\text{min}} \equiv \omega_1$ will be the lowest eigenvalue of the discrete frequency spectrum. Moreover, there will exist only one set of normalizable solutions and so we will suppress the “ α ” label hereafter. By defining $d\tilde{r} = (2M)^{-1} \sqrt{h^s(r)/f^s(r)} dr$, we can write Eq. (3.3) as

$$-\frac{d^2\psi_{\omega l}}{d\tilde{r}^2} + 4M^2 V_{\text{eff}}^s[\tilde{r}(r)]\psi_{\omega l} = 4M^2\omega^2\psi_{\omega l}. \quad (4.4)$$

The function $\tilde{r}(r)$ is a growing monotonic function. At the star core (and choosing properly the integration constant) we have $\tilde{r}|_{r \approx 0} \approx (r/M)/(3\sqrt{F(R)} - 1)$ and the scattering potential becomes

$$V_{\text{eff}}^s(\tilde{r})|_{\tilde{r} \approx 0} \approx \frac{l(l+1)}{4M^2\tilde{r}^2} + C^2 + \mathcal{O}(\tilde{r}), \quad (4.5)$$

where

$$C^2 = \frac{G(R)^2}{2M^2} \left[\frac{(mM)^2}{2} + \frac{M^3 l(l+1)}{R^3 G(R)} + \frac{M^3}{R^3 G(R)} - \frac{M^3}{R^3} \right] \quad (4.6)$$

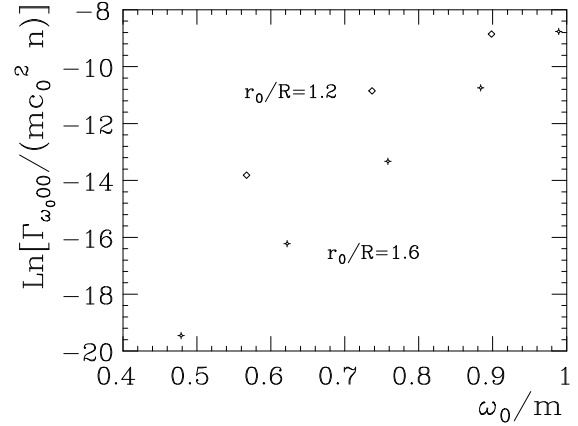


FIG. 10. We plot the detection rate $\Gamma_{\omega_0 00}$ for the eigenfrequencies $\omega_0/m < 1$ assuming observers at different points r_0 . We note that the damping in the detection rate is steeper for observers at weak gravitational potentials. (Here $mM = 2$ and $R/R_c = 1.2$.)

is a positive-definite constant and $G(R) \equiv -1 + 3\sqrt{F(R)}$. Thus, close to the star center, $\psi_{\omega l}$ is proportional to $2M\nu\tilde{r}j_l(2M\nu\tilde{r})$ (since the solutions proportional to $2M\nu\tilde{r}n_l(2M\nu\tilde{r})$ are non-normalizable), where $j_l(x)$ is the spherical Bessel function and $\nu \equiv \sqrt{\omega^2 - C^2}$. Moreover, far away from the star, $V_{\text{eff}}^s(r) \approx m^2$. Hence

$$\psi_{\omega l}(\tilde{r}) \approx A_{\omega l} \begin{cases} B_{\omega l} 2M\nu\tilde{r}j_l(2M\nu\tilde{r}) & (\tilde{r} \approx 0) \\ C_{\omega l} e^{-2iM\tilde{\omega}\tilde{r}} + e^{2iM\tilde{\omega}\tilde{r}} & (\tilde{r} \gg 1) \end{cases} \quad (4.7)$$

where we recall that $\tilde{\omega} \equiv \sqrt{\omega^2 - m^2}$. For $\omega \geq m$, the modes are asymptotically free states and they can be normalized through Eqs. (3.13)-(3.14). Indeed we find $A_{\omega l} = (2\sqrt{\omega\tilde{\omega}})^{-1}$ and $|C_{\omega l}| = 1$. For $\omega_i < m$, the normal modes fade exponentially and $|C_{\omega_i l}| = 0$, where we are using here latin indices i, j, \dots to label the discrete eigenfrequencies. The bounded states should be Klein-Gordon orthonormalized by imposing Eqs. (3.13)-(3.14) except for the fact that in this case $\delta_{AA'} \equiv \delta_{ll'}\delta_{mm'}\delta_{\omega_i\omega_j}$. Thus, we find

$$\int_0^{+\infty} d\tilde{r} |\psi_{\omega_i l}(\tilde{r})|^2 = \frac{\pi}{4M\omega_i^2}. \quad (4.8)$$

The valid set of discrete eigenfrequencies ω_i is determined numerically [10]. Shortly, the strategy consists in evolving solutions with $\psi_{\omega_i l}(0) = 0$ [see Eq. (4.7)] (and arbitrary $\psi'_{\omega_i l}(\tilde{r})|_{\tilde{r}=0} = \text{const.}$) and search for the ω_i 's such that far enough from the star $\psi_{\omega_i l} \sim e^{-2M\sqrt{m^2 - \omega_i^2}\tilde{r}}$ as

	$\omega_{\min}^{\text{class}}/m$	ω_1/m	ω_2/m	ω_3/m	ω_4/m
$mM = 2, R/R_c = 1.2$	0.264	0.351	0.456	0.556	0.648
$mM = 2, R/R_c = 2.0$	0.618	0.679	0.757	0.826	0.874

TABLE I. We list the lowest eigenfrequencies $\{\omega_1, \dots, \omega_4\}$ for different star parameters. The lowest eigenfrequency ω_1 is to be compared with the minimum classical energy $\omega_{\min}^{\text{class}}$. We see that $\omega_{\min}^{\text{class}} \leq \omega_1$, as expected, in the “high-frequency” regime $\omega^{\text{class}} \gg M/R^2$. By assuming that $mM = 2$, then $M/R^2 = 0.07m$ and $M/R^2 = 0.02m$ for $R/R_c = 1.2$ and $R/R_c = 2$, respectively.

ruled by Eq. (4.7) for $\omega_i < m$. In Tab. I we present the lowest eigenfrequencies $\{\omega_1, \omega_2, \omega_3, \omega_4\}$ (normalized by m) for some star parameters. For sake of comparison, we also show the minimum energy value $\omega_{\min}^{\text{class}}$ for a classical particle obtained according to General Relativity when it is static at the star center. Namely, $\omega_{\min}^{\text{class}} = m\sqrt{f(r)}|_{r=0} = (m/2)(3\sqrt{1-2M/R} - 1)$. In the “high-frequency” regime, $\omega^{\text{class}} \gg M/R^2$, where the behavior of classical and quantum particles can be compared, we expect $\omega_i \geq \omega_{\min}^{\text{class}}$ because of the extra intrinsic “kinetic energy” of quantum origin (see Tab. I).

The massive scalar field can be cast as in Eq. (3.15)

$$\hat{\Phi}(x) = \sum_{l=0}^{+\infty} \sum_{m=-l}^l \int_{\omega}^{\omega} [\hat{a}_{\omega lm} u_{\omega lm}(x) + \text{H.c.}], \quad (4.9)$$

where the summation in α was suppressed and we integrate over the free states ($\omega \geq m$) and sum over the eigenfrequencies of the bounded states ($\omega_i < m$). Here

$$[\hat{a}_{\omega lm}, \hat{a}_{\omega' l' m'}^\dagger] = \delta_{AA'}, \quad (4.10)$$

where $\delta_{AA'} \equiv \delta_{ll'} \delta_{mm'} \delta(\omega - \omega')$ and $\delta_{AA'} \equiv \delta_{ll'} \delta_{mm'} \delta_{\omega\omega'}$ for free and bounded states, respectively.

Next we couple [see Eq. (2.8)] the massive scalar field to an Unruh-DeWitt detector characterized by the density of states (2.7). The amplitude (at the tree level) associated with the detection of a bounded state with quantum numbers ω_i, l and m is $\mathcal{A}_{\omega_i lm}^{\text{det}} = \langle 0 | \otimes \langle E | \hat{S}_I | E_G \rangle \otimes | \omega_i l m \rangle$. The detection rate (detection probability per detector proper time) is, thus,

$$\begin{aligned} \Gamma_{\omega_i lm} &= \frac{1}{s_d^{\text{tot}}} \int_0^{+\infty} dE \beta_{E_0}(E) |\mathcal{A}_{\omega_i lm}^{\text{det}}|^2 \\ &= 2c_0^2 n \sqrt{f^s(r_d)} \frac{|\psi_{\omega_i l}(r_d)|^2}{r_d^2} |Y_{lm}(\theta_d, \varphi_d)|^2, \end{aligned} \quad (4.11)$$

where again the detector selectivity was chosen such that $\langle E | m(0) | E_G \rangle \equiv 1$ and we have tuned the energy gap of

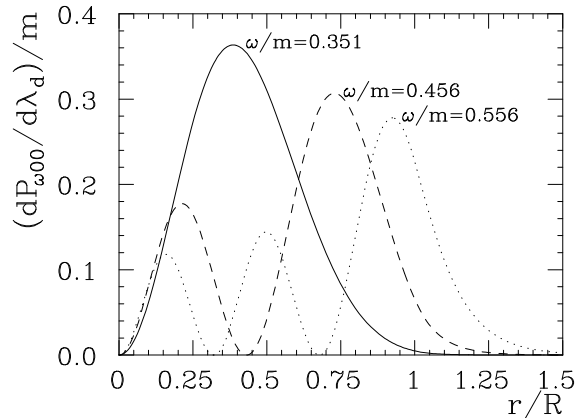


FIG. 11. The probability density $(d\mathcal{P}_{\omega_{00}}/d\lambda_d)/m$ is plotted for the three lowest eigenfrequencies when $mM = 2$ and $R/R_c = 1.2$. The smaller the ω/m ratio, the closer to the star center the particle is.

the detector as usually: $E_0 = \omega_i/\sqrt{f^s(r_d)}$. [Notice the resemblance of Eqs. (4.11) and (3.17), where we recall that $\dim(\psi_{\omega_i l}/\psi_{\omega_l}^\alpha) = \dim(\sqrt{\omega})$.] (The detection of free states follows as previously [see, e.g., Eq. (2.10)].) As in the Reissner-Nordstrom case, we can calculate the detection rate $\Gamma_{\omega_0 lm}$ in the special case where the massive state $|\omega_0 lm\rangle$ is defined by an experimentalist lying on the detector, as shown in Fig. 10.

By using Eq. (4.11), we can define a normalized probability density $d\mathcal{P}_{\omega_i lm}/dV_d$ analogously to Eq. (3.18), where $dV_d = d\lambda_d r_d^2 \sin\theta_d d\phi_d$ and $d\lambda_d = \sqrt{h^s(r_d)} dr_d$. The proper radial distance can be integrated from the center of the star as a function of the radial coordinate leading to

$$\begin{aligned} \lambda &= \frac{\arcsin[\sqrt{2Mr^2/R^3}]}{\sqrt{2M/R^3}} \Theta[R-r] + \left\{ \frac{\arcsin[\sqrt{2M/R}]}{\sqrt{2M/R^3}} \right. \\ &+ M \ln \left[\frac{r + r\sqrt{1-2M/r-M}}{R + R\sqrt{1-2M/R-M}} \right] + r\sqrt{1-\frac{2M}{r}} \\ &\left. - R\sqrt{1-\frac{2M}{R}} \right\} \Theta[r-R]. \end{aligned} \quad (4.12)$$

The radial-distance probability density $d\mathcal{P}_{\omega_i lm}/d\lambda_d$ is then calculated analogously to Eq. (3.20). In Fig. (11), we plot $d\mathcal{P}_{\omega_i lm}/d\lambda_d$ for particles with different ω_i/m ratios. The mean particle radial distance $\langle \lambda_d \rangle$ is defined analogously to Eq. (3.21) and was calculated numerically as shown in Fig. (12).

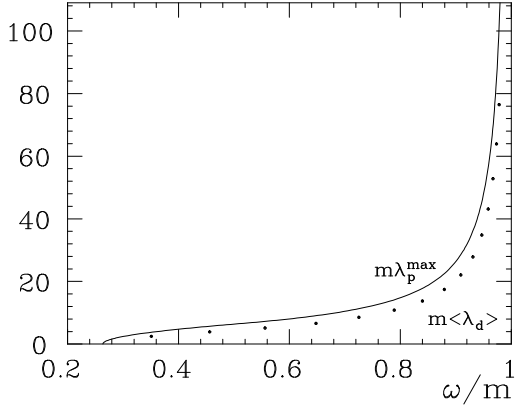


FIG. 12. $\langle \lambda_d \rangle$ is plotted for various eigenfrequencies assuming $l = 0$, $mM = 2$ and $R/R_c = 1.2$. We note that $\langle \lambda_d \rangle < \lambda_p^{\max}$, as expected, in the “high-frequency” regime $\omega^{\text{class}}/m \gg (M/R^2)/m$. (Here $\omega_{\text{min}}^{\text{class}}/m = 0.264$, $\omega_1/m = 0.351$ and $(M/R^2)/m = 0.07$.)

Now, by taking a procedure analogous to the one used in the black hole case [see Eq. (3.22)], we find that a classical particle with total energy $\omega < m$ (as measured by static asymptotic observers) will be at $r_p \leq r_p^{\max}$, where

$$r_p^{\max} = \sqrt{\frac{R^3}{2M} \left[1 - \left(3\sqrt{F(R)} - 2\frac{\omega}{m} \right)^2 \right]} \Theta \left[\sqrt{F(R)} - \frac{\omega}{m} \right] + \frac{2M}{1 - (\omega/m)^2} \Theta \left[\frac{\omega}{m} - \sqrt{F(R)} \right]. \quad (4.13)$$

Because the proper radial distance $\lambda = \lambda(r)$ is again a growing monotonic function [see Eq. (4.12)], we have once more $\lambda_p \leq \lambda_p^{\max} \equiv \lambda(r_p^{\max})$. This is compared with $\langle \lambda_d \rangle$ in Fig. (8). We see that $\langle \lambda_d \rangle < \lambda_p^{\max}$, as expected, in the “high-frequency” regime, $\omega^{\text{class}} \gg M/R^2$.

V. CONCLUSIONS

The detection rate for massive particles with total energy $E < mc^2$ was calculated for the Rindler wedge, black holes and star spacetimes. The mean particle positions were calculated and shown to be in qualitative agreement with General Relativity predictions in the “high-frequency” regime. The observation process is naturally taken into account in the formalism by considering Unruh-DeWitt-like detectors. In this way, we clearly define what we mean by “observing a particle”.

Although it is possible, in principle, to measure particles satisfying Eq. (1.1) even at Earth, these events are so rare in such weak gravitational fields that do not have to be considered for practical purposes. This can be seen from the analysis of the scattering potential [see discussion below Eq. (4.3)].

Notwithstanding the consideration of massive particles with *arbitrary small* total energy is just fundamental for a comprehensive understanding of some phenomena occurring in highly curved spacetimes (e.g., black holes) and accelerated frames. For example, the weak decay of uniformly accelerated protons in the Minkowski vacuum which is described by the $p \rightarrow n e^+ \nu$ channel (at the tree level) in an inertial frame was shown to be representable by the combination of the following three channels: $p e^- \rightarrow n \nu$, $p \bar{\nu} \rightarrow n e^+$ and $p e^- \bar{\nu} \rightarrow n$, in the proton coaccelerated frame. According to this description, the proton would decay by the absorption of a Rindler e^- and/or $\bar{\nu}$ from the Fulling-Davies-Unruh thermal bath “attached” to the proton proper frame. However, in order that inertial and noninertial frame descriptions lead to the same observables (e.g. proper lifetime), we emphasize that the energy spectrum of the (massive) Rindler e^- ’s and e^+ ’s must be $\omega \in [0, +\infty)$ (despite Rindler e^- ’s and e^+ ’s have mass $m \approx 0.5$ MeV, as usually) [1]. Perhaps an even more extreme case concerns the importance of *zero-energy* particles to understand the radiation emitted from uniformly accelerated charges according to comoving observers. Namely, the emission of a (usual) Minkowski photon with transverse momentum \mathbf{k}_\perp from a uniformly accelerated charge as described by inertial observers corresponds, according to coaccelerated observers, to either the *absorption from* or the *emission to* the Fulling-Davies-Unruh thermal bath of a zero-energy photon with the same transverse momentum \mathbf{k}_\perp . For obvious reasons, in Ref. [11] the photons considered were supposed to be massless but the same conclusion in terms of zero-energy particles would hold even if we considered that the photons were *massive*.

Acknowledgements

We are indebted to Professor L. Parker for reading the manuscript. We are grateful to Dr. A. Gammal for calling our attention to Ref. [10]. One of us (D.V.) is thankful to Drs. A. Higuchi and B. Kay for conversations on this issue. We acknowledge Fundação de Amparo à Pesquisa do Estado de São Paulo for supporting J.C. (fully) and D.V. (partially) and Conselho Nacional de Desenvolvimento Científico e Tecnológico for supporting G.M. (partially). This work was supported in part by the US National Science Foundation under Grant: No PHY-0071044.

-
- [1] G. E. A. Matsas and D.A.T. Vanzella, Phys. Rev. D **59**, 094004 (1999). D. A. T. Vanzella and G. E. A. Matsas Phys. Rev. Lett. **87**, 151301 (2001).
 - [2] J. L. Friedman, Commun. Math. Phys. **62**, 247 (1978).
 - [3] N. D. Birrell and P. C. W. Davies, *Quantum Field Theory in Curved Spacetime* (Cambridge University Press, Cambridge, England, 1982).
 - [4] S. A. Fulling, *Aspects of Quantum Field Theory in Curved Space-Time*, (Cambridge University Press, Cambridge, 1989).
 - [5] W. G. Unruh, Phys. Rev. D **14**, 870 (1976). B. S. DeWitt, *General Relativity*, eds. S.W. Hawking and W. Israel (Cambridge University Press, Cambridge, 1979).
 - [6] J. Castineiras and G. E. A. Matsas, Phys. Rev. D **62**, 064001 (2000).
 - [7] A. Higuchi, G. E. A. Matsas, and D. Sudarsky, Phys. Rev. D **56**, R6071 (1997).
 - [8] R. M. Wald, *General Relativity*, (University of Chicago Press, Chicago, 1984).
 - [9] D. A. T. Vanzella and G. E. A. Matsas Phys. Rev. D **61**, 127303 (2000).
 - [10] N. J. Giordano, *Computational Physics*, (Prentice-Hall, Upper Saddle River, 1997).
 - [11] A. Higuchi, G. E. A. Matsas, and D. Sudarsky, Phys. Rev. D **45**, R3308 (1992).